Statics and Dynamics of Polymeric Melts: A Numerical Analysis†

Kurt Kremer

Institut für Festkörperforschung der Kernforschungsanlage Jülich GmbH, D-5170 Jülich, West Germany. *Received December 21, 1982*

ABSTRACT: The static and dynamic properties of polymeric melts are analyzed by an extended Monte Carlo simulation of self-avoiding walks (SAWs) on the diamond lattice for chain lengths up to 200 steps. For the static properties we find that the mean square end-to-end distance for melts at concentrations $c \rightarrow 1$ is equal to the result for a single chain at $T = \Theta$, the Θ temperature. We choose conditions where SAW effects on the polymer configurations are screened out over distances much smaller than the coil radius. Neither the dynamic structure function $S(k,t)$ nor the mean square displacements of inner monomers show any onset of reptation but are well accounted for by the Rouse model. Reptation is only found for a system where all chains except one were frozen in. But it also turns out here that recent theories can describe our results only qualitatively.

I. Introduction

Dense systems of long flexible polymers show a significantly different physical behavior compared to the single chain in very dilute solution. The static properties of a single chain in solution now seem to be rather well understood theoretically and experimentally (ref 1 and 2 and references therein). Much more complicated is the situation in polymeric melts. Especially, the dynamics of melts, where the chains are strongly entangled, is still poorly understood.[3] The dynamics of a single chain is, in the so-called free-draining limit, well described by Rouse dynamics.[4,5] There exist several approaches of modifying this model in order to take into account the increasing number of entanglements.[6] However, all these theories[6] increase the local friction and do not take into account the topological character[7] of the entanglements, which means that no two bonds are allowed to cross each other during a possible motion. A very different approach now is given by the reptation model.[8,9] Here, the topological character of the entanglements is considered in the following way. Due to the restrictions of the other chains a single chain only can move through a "tube"[8] built of fixed obstacles by the surrounding monomers. The crucial point in this theory is the assumption that the fluctuations or the mobility of this randomly shaped tube is much lower compared to the motions of the single chain itself (see, e.g., ref 10). Although it is not clear up to now how and if the crossover from a less dense system with "fast-moving obstacles" to the dense system with "fixed obstacles" occurs, most of the later theoretical and experimental work[10–12] is based on this model. However, there are numerical investigations of dense polymer systems with rather short chains which do not show any crossover to reptative behavior.[13,14] Analogously, spin-echo neutron scattering studies of poly(dimethylsiloxane) (PDMS) melts[15] do not show reptation. On the other hand, de Gennes and Lêger[16] claimed that the chains in these studies are still too short to be entangled and to show reptation. In addition, a new NMR investigation of the dynamics of a polymeric melt[17] used the Rouse model to explain the results.

Therefore it seems to be useful to present an extended numerical investigation in which all conditions for reptation to occur, known up to now, are fulfilled. We want to check whether reptation occurs in such a system or not. This investigation then also can clearly show the shortcomings of a recent Monte Carlo investigation[18] that claims to find the reptation behavior.

† This paper is in partial fulfillment of the requirements for the Ph.D. Thesis at the University of Cologne.

In order to fulfill the mentioned conditions, at first we have to analyze very carefully the static properties of our dense system compared to other systems. In this context a connection to the Θ-point behavior of polymers is analyzed. This is done in section III, while in section II the model used and the Monte Carlo algorithm are explained. In section IV the dynamics is investigated, and section V contains the conclusions.

II. Model and Monte Carlo Methods

To test the predictions of the reptation model, one has to use many long chains at high density. In order to reach this aim it is necessary to use a lattice model. In the present work the diamond lattice is used. The chains are then modeled by self-avoiding walks (SAW) that are confined to the lattice. This SAW consists of N bonds connecting $N + 1$ monomers which sit on the lattice sites. Besides the SAW condition, which means that no site can be occupied by more than one monomer, no further interaction is considered. The concentration, which is a difficultly determined quantity for off-lattice systems,[13] is simply defined by the mean number of monomers per lattice site. The length l of each bond is given by $l^2 = 3$. For a more detailed description of this model we refer to ref 2 and 19. For the simulation, we use a 3–4 bond motion as described in detail in ref 2 and 19. In addition to the single-chain problem, the special chain in which a motion is attempted is chosen by a random number. This kind of motion obeys Rouse dynamics,[2,19] which means that a microscopic time step τ_0 is given by one attempted motion per bond of our whole system. Entanglement effects are automatically taken into account by the SAW condition, because for the chosen motions no bond cuts during the rotations are possible.[19] Taking this fact into account and noting that simple occupation numbers replace time-consuming distance calculations of the continuum models, it is clear that, for our present computers (IBM 3033), using such a lattice model allows an approximate increase of a factor of 10 in the chain lengths for similar computing times. This results in longer effective chains even if one takes into account that a bond of a lattice polymer (coordination number of the diamond lattice is $q = 4$) represents a lower number of real bonds than a bond of a freely jointed polymer.[13,14] Otherwise one is not able to reach long chains[13] or one cannot test explicitly the entanglement condition.[14]

In the present investigation chain lengths up to $N = 200$ and concentrations up to $c = 0.344$ are used. The smaller systems are only needed for static properties. In order to simulate such a system and to cover all necessary time scales, one has to introduce periodic boundary conditions. For the present system the unit cell is a fcc cube of length

0024-9297/83/2216-1632$01.50/0

$b = 4$ and eight lattice sites with a basis vector (1,1,1). Therefore for cubes with side lengths which are multiples of four, the periodic boundary conditions cause a simple backshifting.[2,19] In order to prevent serious influence due to unphysical self-entantanglements, the length L of the cube must be larger than the chain diameter, which means

$$L > 2\langle R_G^2(N)\rangle^{1/2} \tag{1}$$

where $\langle R_G^2(N)\rangle = \langle (N+1)^{-2}\sum_{i=1}^{N}\sum_{j=i+1}^{N+1}(\vec{r}_i - \vec{r}_j)^2\rangle$, with $\vec{r}_i$ the position of the ith monomer, is the radius of gyration. Then self-entanglements are still possible but have a very small probability, and therefore their influence can be neglected. Because it is complicated to find a starting configuration of SAWs on this lattice, we started with NRRWs (nonreversal random walks). NRRWs are simple random walks where direct self-reversals are forbidden. The lattice was filled up randomly with the desired number of NRRWs with length N. Then each occupied site was registered as occupied with the logical variable "true". During the simulation, after each performed motion, new occupied sites were registered in the same way and *no* new double occupancy was allowed. It turned out that even for the largest system (seven chains with $N = 200$, $L = 32$, and $c = 0.344$), less than 100 successful motions per bond were needed to change the initial NRRW system into a SAW system. This method also seems to be very useful for searching for the properties of very dense systems. The relaxation of the system into equilibrium was controlled by comparing the mean square end-to-end distance of a single chain, $\langle R^2(N)\rangle = \langle(\vec{r}_1 - \vec{r}_{N+1})^2\rangle$, with the mean value of all chains. During the calculations all coordinates of at least one chain were stored in the system by a compact storage algorithm, as described in detail in ref 19. This algorithm uses integers from 0 to 3 for the four possible bonds; therefore an integer 4 number ($\leq 2^{31} - 1$) can contain a sequence of 15 bonds.

III. Static Properties of Melts

For dense polymer systems it is well-known that the exponent of $\langle R^2(N,c)\rangle$ and $\langle R_G^2(N,c)\rangle$ changes over from the SAW behavior ($\nu = 0.59$) to classical behavior ($\nu = {}^1/_2$). This does not mean that the chains then behave as simple random walks ($\langle R^2\rangle = l^2N$), as shown below. Because it is impossible to perform dynamical Monte Carlo calculations at $c = 1$, one has to analyze carefully the above-mentioned crossover. This can be performed by using the scaling theory of Daoud and Jannink.[20] For a given concentration c we can define a screening length ξ. Over distances less than ξ the monomers mainly interact with monomers of the same chain; therefore within this distance the polymer still has its SAW behavior. Using the blob concept,[3] one can say that inside blobs of diameter ξ the chain is expanded; this gives

$$\xi \propto lN_B^{\nu}, \qquad \nu = 0.59 \tag{2}$$

where N_B is the number of monomers in such a blob. For distances larger than ξ the interaction with the other chains screen out the expanding forces. Therefore the mean square end-to-end distance of the whole chain can be described by an ideal chain of N/N_B bonds with bond length ξ

$$\langle R^2(N,c)\rangle \propto l^2N_B^{2\nu}(N/N_B) \tag{3}$$

Of course, this is only valid for $N_B \lesssim N$. The critical concentration c^*, where the region of validity of eq 3 begins, is simply estimated by

$$c^*(N) \approx N/\langle R^2(N)\rangle^{d/2} \propto l^{-d}N^{1-\nu d} \propto N^{-0.77} \qquad (\nu = 0.59,\ d = 3) \tag{4}$$

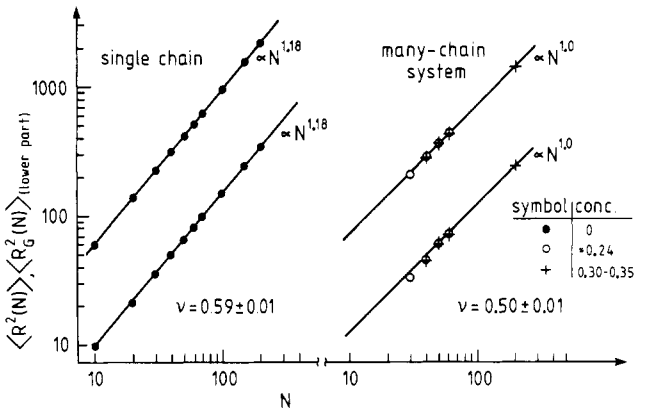

Figure 1. log–log plot of $\langle R^2(N,c)\rangle$ and $\langle R_G^2(N,c)\rangle$ for different concentrations. The data for $c = 0$, taken from ref 2, clearly give $\nu = 0.59$. For the systems at $c = 0.24$, taken from ref 35, and $c = 0.30$–0.344, no distinction within this figure can be made. The data give $\nu = 0.50 \pm 0.1$.

In our case this gives $c^*(N = 50) \approx 0.05$ and $c^*(N = 200) \approx 0.02$. Of course, the exact value of $c^*(N)$ can differ from these estimates by a factor of 2 or 3, but remembering the prefactor of $\langle R^2(N)\rangle$ of a single SAW on this lattice,[2] one can see that the precise value of c^* seems to be lower than the above numbers (see Figure 1). Using these results, one can write the crossover in a scaling form[20]

$$\langle R^2(N,c)\rangle = N^{2\nu}f(c/c^*(N)) = N^{2\nu}f(c/N^{1-\nu d}) \tag{5a}$$

with

$$f(x) \propto \text{constant}, \quad x \to 0 \qquad \propto x^{-(1-2\nu)/(1-\nu d)}, \quad x \gg 1 \tag{5b}$$

which gives

$$\langle R^2(N,c)\rangle \propto Nc^{-0.23} \qquad (d = 3,\ \nu = 0.59) \tag{6}$$

for $c^* \ll c \ll 1$.

Here, we are mainly interested in very dense systems. Therefore the restriction $c \ll 1$, which means $N_B \gg 1$, may not be obeyed. For the diamond lattice one needs $N_B > 20$ to reach the behavior of eq 2.[2] Therefore eq 5 can only be valid for

$$c^* \ll c \ll 0\ (20^{-0.77}) \approx 0.10 \tag{7}$$

With the result $\langle R^2(N = 20)\rangle$ of a free chain of 20 bonds, this boundary is lowered to 0.02. Therefore concentrations of $c > 0.1$ represent very dense systems. For higher concentrations with $N_B \lesssim 20$, it is a very good approximation to use instead of eq 2 the NRRW formula[21] ($q = 4$)

$$\xi^2 = 6N_B - 4.5 \approx 6N_B \tag{8}$$

which gives an effective exponent ν_{eff} between the limits $\nu = {}^1/_2$ and $\nu = 0.59$. After eq 5b this results in a concentration-dependent lowering of the exponent $(1 - 2\nu)/(1 - \nu d)$. Table I gives the results of different systems, and Figure 1 shows a log–log plot of $\langle R^2(N,c)\rangle$ and $\langle R_G^2(N,c)\rangle$ compared to the $c = 0$ case. For concentrations $c \approx 0.24$ and $c \approx 0.30$–0.35, there is no significant difference in the data. One clearly finds the exponent $\nu \approx {}^1/_2$, in agreement with others.[25,26] In Figure 2 we try to extrapolate $\langle R^2(N,c)\rangle/N$ to $c \to 1$. The data show, as expected, a c-dependent decrease in slope. A similar decrease, smaller than the scaling prediction, was also found by other authors for various systems of shorter chains.[22,27-29] For the extrapolation to $c = 1$ we first find a trivial lower bound, the NRRW result, which gives for a lattice with coordination number $q = 4$ just $\langle R^2(N)\rangle/N \to 2l^2$. This is a lower

Table I
Results for Systems with Concentration $c \geq 0.30$[a]

N	NC	L	c	$\langle R^2(N,c)\rangle$	$\langle R_G^2(N,c)\rangle$
40	8	20	0.32	280 ± 2	45.1
50	6	20	0.30	365 ± 5	59.7
60	5	20	0.30	438 ± 5	71.8
200	7	32	0.344	1500 ± 30	255 ± 5
200	7	32	0.344	1465 ± 30[b]	245 ± 5[b]

[a] N gives the number of monomers and NC the number of chains of the special system in the box of size L^3 with periodic boundary conditions. Further data, used in Figures 1 and 2, are only used to clarify the situation. These data were calculated for further purposes.[19,35] [b] Results of the single mobile chain of 200 bonds in a frozen environment of other 200-bond chains. Because the environment is built by the same chains, no significant change in $\langle R^2\rangle$ and $\langle R_G^2\rangle$ occurs.

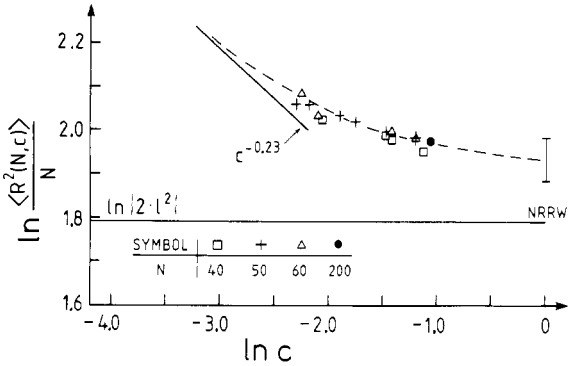

Figure 2. Double-logarithmic plot of $\langle R^2(N,c)\rangle/N$ vs. concentration c to estimate the value at $c \to 1$. The straight line gives the desired slope after eq 6 for $N_B \gg 1$ (for this lattice we need $N_B > 20$). The horizontal line gives the trivial lower boundary of the NRRW result, where the error bar at $\ln c = 0$ gives the estimated uncertainty of $\langle R^2(N,c=1)\rangle$. To clarify the picture further, data at lower concentration[19,35] are included.

bound because the effect of forbidden direct self-reversals can never be screened out by the interaction with other chains. Similarly, the shortest closed loop also is never allowed and so forth. Therefore one should expect a somewhat higher amplitude at $c = 1$. These arguments are in good agreement with other results[26,27] and the extrapolation of Figure 2:

$$(\langle R^2(N,c)\rangle/N) \xrightarrow[N\to\infty]{c\to 1} 6.5 \pm 0.2 \qquad (9)$$

Using a similar argument, one can find the Θ-point behavior[2] during the collapse transition of a single chain. Using those results for the same lattice (Figure 6 of ref 2), one finds

$$\langle R^2(N,T=\Theta)\rangle/N \xrightarrow{N\to\infty} 6.60 \pm 0.05 \qquad (10)$$

This gives

$$\langle R^2(N,c=1)\rangle/N \approx \langle R^2(N,T=\Theta)\rangle/N = 2.20l^2 \qquad (11)$$

while the simple random walk would give $\langle R^2\rangle = l^2N$. Equation 11 is in excellent agreement with experimental results[23] and shows that one has to distinghish between the simple random walks, NRRWs, and chains at $T = \Theta$ and $c \to 0$ or $T = \infty$ and $c \to 1$ even in statics.

A recent simulation[24] of a polydisperse system of shorter chains at $c = 1$ claims to find $\nu = 0.51$ at $c = 1$ (similar to ref 29). The above results are not able to distinguish clearly between $\nu = 0.50$ and 0.51, but we think that this result is an effect of the polydispersity and the shortness of the chains.

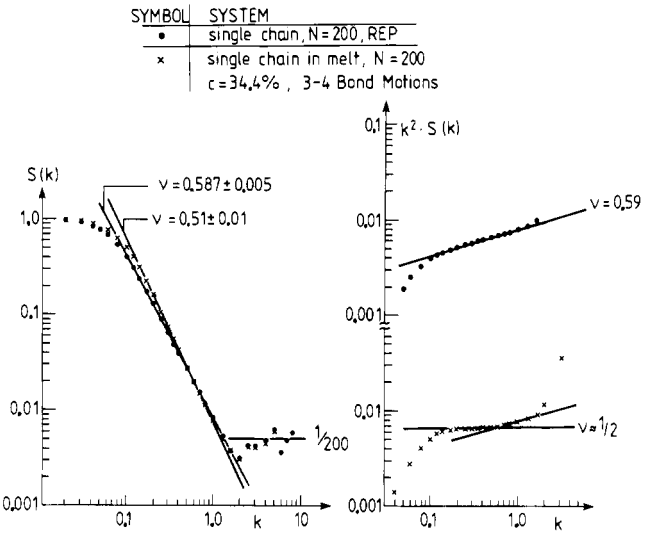

Figure 3. Coherent static structure function $S(k)$ and $k^2S(k)$ (eq 12) of a single chain of 200 bonds at $c = 0$ calculated by the reptation alogorithm[2] and of a chain in a melt of the same chains (all chains moving) ($N = 200$) at $c = 0.344$. For $2\pi\langle R_G^2\rangle^{-1/2} < k < 2\pi l^{-1}$ one expects $S(k) \propto k^{-1/\nu}$. The single free chain shows $\nu = 0.59$ in the range $0.1 < k < 1.5$. The chain in the melt clearly shows a blob boundary at $k \approx 0.65$. For large k the desired scattering around $1/N$ is reached.

For our largest system (seven chains with $N = 200$, $L = 32$, and $c = 7(N+1)/(L^3/8) = 0.344$), which is used later for analyzing dynamics, N_B is directly calculated via the coherent structure function $S(k)$ of a single chain in the melt of moving chains. $S(k)$ is given by

$$S(k) = \frac{1}{(N+1)^2}\left\langle \left| \sum_{j=1}^{N+1} \exp(i\vec{k}\cdot\vec{r}_j) \right|^2 \right\rangle_{|\vec{k}|} \qquad (12)$$

The index $|\vec{k}|$ means that $S(k)$ is an average over all directions of $\vec{k}$ in order to avoid Bragg peaks and to calculate melt results.[2] In Figure 3 the result is shown in comparison to the data of a single free 200-bond chain. The free SAW clearly shows $\nu = 0.59$ for wave vectors k within $0.1 < k < 2.0$, which means that over distances λ, $2\pi/0.1 > \lambda > 2\pi/2.0$, the chain behaves as an SAW. This is the range of lengths from the whole chain diameter down to a few bonds. For the chain in the melt, the figure shows a very different behavior. Up to $k \leq 0.65$, we find $\nu = 1/2$, which means that for distances larger than $\lambda_B = 2\pi/0.65$, the chain behaves as an ideal one. For $\lambda < 2\pi/0.65$, we find an increasing exponent ν_{eff}; the SAW structure becomes dominant. This means that the diameter $d_B = \xi$ of the blobs is given by

$$d_B \approx \lambda_B = 2\pi/k_B \approx 10 \qquad (13)$$

Using eq 8, we arrive at $N_B \approx 16$. This is a somewhat higher value than expected from eq 4 and 8 ($N_B \approx 10$), which seems to be an effect of the fluctuations in the system, because all chains are moving. Concerning this result ($N > 10N_B$), we can claim that the system of chains with 200 bonds at $c = 0.344$ really represents a dense polymeric system.

IV. Dynamic Properties of Melts

For analyzing dynamical aspects of polymeric melts *only*, the largest system of 200-bond chanins is used. As mentioned in the Introduction, up to now there exist, in principle, two models for chain dynamics. The first one is the Rouse model, which should hold in the so-called free-draining limit. The second one is the reptation model, which is often[10-12,18] expected to hold for dense systems.

Here, we want to clarify whether a crossover from Rouse dynamics to reptation dynamics occurs for the available systems. First we look at the mean square displacements of an inner monomer, which is averaged over 20 monomers in order to reduce statistical scatter

$$g_1(t) = \frac{1}{20}\sum_{i=91}^{110} \langle [\vec{r}_i(t_0 + t) - \vec{r}_i(t_0)]^2 \rangle \tag{14}$$

and the corresponding displacements where the center-of-mass ($\vec{r}_s$) motion is separated out

$$g_2(t) = \frac{1}{20}\sum_{i=91}^{110} \langle \{(\vec{r}_i(t_0 + t) - \vec{r}_s(t_0 + t)) - (\vec{r}_i(t_0) - \vec{r}_s(t_0))\}^2 \rangle \tag{15a}$$

Later on we also analyze the motion of the center of mass itself, which is measured by

$$g_3(t) = \langle [\vec{r}_s(t_0 + t) - \vec{r}_s(t_0)]^2 \rangle \tag{15b}$$

The Rouse model now predicts the following behavior:[4] At very short times t, g_1 and g_2 show the diffusion of a single monomer until g_1 and g_2 reach distances of $\mathcal{O}(l^2)$, where the monomer cannot diffuse freely any longer due to the chain constraint. Therefore we have

$$g_1(t) \approx g_2(t) \propto t, \qquad g_1, g_2 < l^2 \tag{16}$$

At longer times the chain relaxation is dominant, which gives

$$g_1(t) \approx g_2(t) \propto t^{1/2} \tag{17}$$

until $g_1(t)$ reaches approximately $\langle R_G^2(N,c) \rangle$. Then the whole chain diffuses, which results in

$$g_1(t) \propto t \qquad g_1(t) > \langle R_G^2(N,c) \rangle$$

$$g_2(t) \propto \text{constant} \qquad g_1(t) > \langle R_G^2(N,c) \rangle \tag{18}$$

For the reptation model a very different prediction is given by de Gennes.[10] Here, we give a short explanation of the different power laws similar to those in ref 10 and 37. Equation 17 holds until $g_1(t)$ reaches d_T^2, the tube diameter. Orginally it was thought that the tube diameter is nothing other than the blob diameter d_B of section III. If we assume that $d_T \approx d_B$[30] (but perhaps the tube diameter is larger),[16,31] the typical entanglement length N_e of the reptation model is of the order of N_B, the number of monomers per blob. After g_1 and g_2 reach d_T^2, typcial configurations (de Gennes "defects") inside a blob, or between two entanglement points, can only relax by diffusion along the tube. This Rouse relaxation of of defects along the tube, which itself is a random walk, leads to

$$g_1(t) \approx g_2(t) \propto t^{1/4} \tag{19}$$

After the "defects" relax along the chain in the tube, the chain is still in the original tube. Now each single monomer, just as the whole chain and therefore also the center of mass, diffuses along the same tube, which gives

$$g_1(t) \propto t^{1/2}$$

$$g_2(t) \propto \text{constant} \tag{20}$$

After the chain leaves the original tube one can speak of a free but very slow diffusion of the whole chain:

$$g_1(t) \propto t$$

$$g_2(t) \propto \text{constant} \tag{21}$$

Figure 4 summarizes the behavior of $g_1(t)$ as expected by the reptation model.[10] Because $N_e \approx N_B = 10$–16, all conditions up to now known necessary for the validity of the reptation model are fulfilled. Of course, if d_T were much larger than d_B, one always could argue that the regime of reptation is not yet reached.

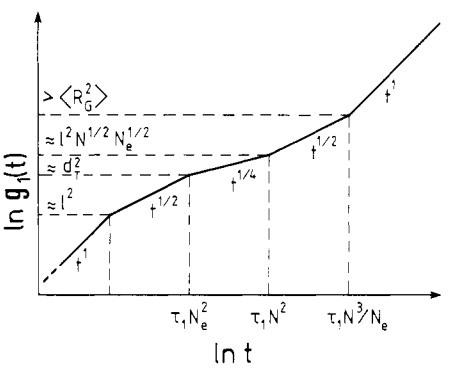

Figure 4. Schematic picture of the mean square displacements of inner monomers as calculated by de Gennes.[11] $\tau_1 N^2$ often is called τ_d, and $\tau_1 N^3/N_e \equiv \tau_R$, the tube renewal time.

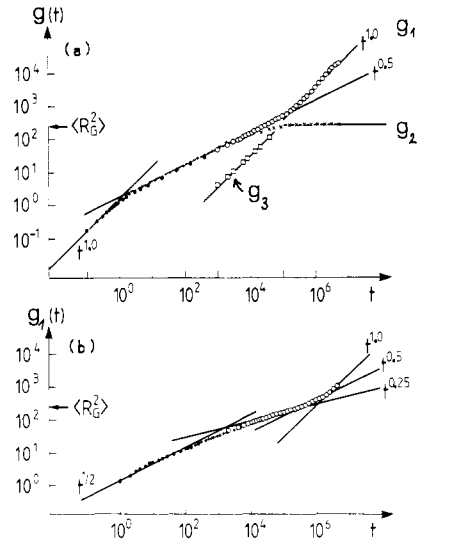

Figure 5. log–log plot of $g_1(t)$ vs. time t in units of the microscopic time constant τ_0 for $N = 200$. (a) Chain in a melt of the same chains at $c = 0.344$. The different symbols for $g_1(t)$ are due to independent runs covering different time scales. Where possible, results for g_2 and g_3 are included. (b) Single mobile chain in a frozen environment of the same chains at $c = 0.344$. Here, the different symbols represent independent runs for varying time scales with different environment configurations.

Due to the chosen algorithm of motion, which obeys Rouse dynamics for a free NRRW[2,19] on this lattice, we can define a fundamental time step τ_0 by one attempted motion per monomer. To cover the whole time scale, up to 10^7 time steps were performed for the system where all chains were moving. Figure 5a shows the results for $g_1(t)$; parts of $g_2(t)$ and $g_3(t)$ are, where possible, included. The data start with the diffusion of the single monomer; then $g_1(t)$ shows for 5 decades Rouse behavior until $g_1(t)$ reaches distances of about $\langle R_G^2(N) \rangle$. Then $g_2(t)$ becomes a constant, and $g_1(t)$ shows the diffusion of the whole chain. This is in excellent agreement with the Rouse model and no onset of reptation can be seen.

To establish the characteristics of reptation in such a system, we also study the case where six of the long chains were frozen in and only the seventh chain was allowed to move. Using a corresponding time scale, we now, apart from the initial t^1 law, find all the different regimes of $g_1(t)$, as predicted by the reptation model (Figure 5b). Figure 6 shows the results for the single moving chain in the frozen system in more detail. Here, for $t > 10^4$ it is possible to distinguish between $g_1(t)$ and $g_2(t)$. Just as predicted

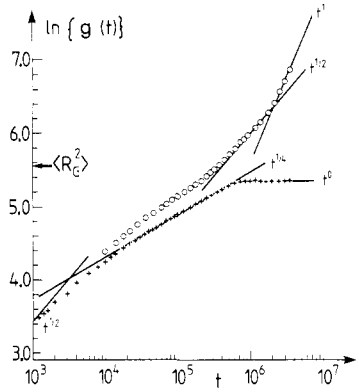

Figure 6. More detailed picture of the results of Figure 5b for $g_1(t)$ and $g_2(t)$. Here, the different runs are not distinguished.

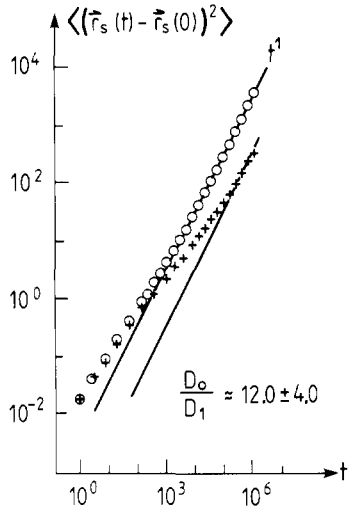

Figure 7. log–log plot of the mean square displacements $g_3(t)$ vs. time t for the chain in the melt (○) and the chain in the frozen environment (+). D_0/D_1 gives the estimated ratio of the diffusion constants.

by eq 19–21, $g_2(t)$ clearly shows the $t^{1/4}$ behavior for nearly 2 decades until $g_1(t)$ shows the crossover into the second $t^{1/2}$ regime, where $g_2(t) \approx$ constant. Comparing all these results with $g_3(t)$, which is shown in Figure 7, we find complete consistency. For $t \leq 5 \times 10^2$, $g_3(t)$ for both the chain in the totally mobile system and the chain in the frozen environment concide. 5×10^2 is just the time where $g_1(t)$ in the case of Figure 5b begins to recognize the tube walls, which results also in a decrease of the motion of thee center of mass. We now can calculate N_e using the results of Figures 4 and 6. This gives

$$N_e \approx 13 \pm 3 \tag{22a}$$

from the length of the $t^{1/4}$ regime of $g_1(t)$ in Figure 6,

$$N_e \approx 50 \pm 10 \tag{22b}$$

analogously from the second $t^{1/2}$ regime,

$$N_e \approx 20 \pm 5 \tag{22c}$$

analogously from the $t^{1/4}$ and $t^{1/2}$ regime together, and

$$N_e \approx 9 \pm 1 \tag{22d}$$

from $g_1(\tau_1 N_e^2)$. These results show the more quantitative character of the above-mentioned estimates of de Gennes.[10] Indeed, even for a frozen environment we expect along a chain fluctuation on the local d_T etc., while in the theory,[10] d_T enters as an average effective quantity only.

Because the functions $g_1(t)$ and $g_3(t)$ can in real experiments only be measured directly in their diffusive time

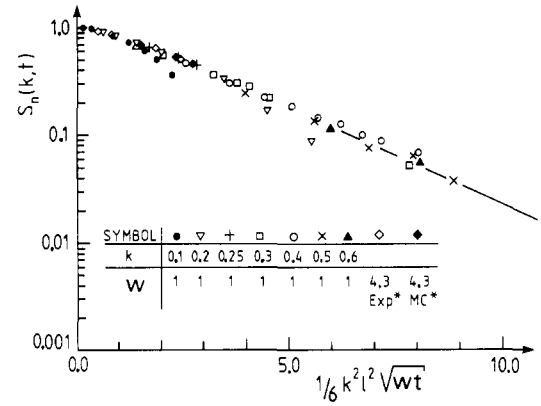

Figure 8. $S_n(k,t)$ after eq 23 and 25 for the completely mobile system in a semilogarithmic plot vs. the variable $^1/_6 k^2 l^2 (wt)^{1/2}$. The fit parameter w is set to 1 for the present data. For the included experimental and Monte Carlo data of ref 33, we needed $w = 4.3$. These data were taken from Figure 1 of ref 33. For a detailed comparison of these experimental and Monte Carlo data we refer to this paper.[33]

limit ($t \to \infty$), it is useful to consider also the time-dependent structure function $S(k,t)$ of a single chain

$$S(k,t) = \frac{1}{(N+1)^2} \langle \sum_{i=1}^{N+1} \sum_{j=1}^{N+1} \exp\{i\vec{k}\cdot(\vec{r}_i(t+t_0) - \vec{r}_j(t_0))\}\rangle_{|\vec{k}|} \tag{23}$$

This structure function can in a normalized form

$$S_n(k,t) = S(k,t)/S(k,0) \tag{24}$$

directly be measured by neutron spin-echo methods.[15] For the unrestricted Rouse model, one gets[32]

$$S_n(k,t) = f(l^2k^2(wt)^{1/2}/6),$$
$$kl/2\pi < 1; \quad wt \gg 1$$
$$f(x) \propto \exp(-x), \quad x \gg 1 \tag{25}$$

where w is a microscopic jump rate. Here, we set $w = 1$ and use it as a fit parameter while comparing our results to other results. Equation 25 only holds for the ideal Rouse case. Here, we have to restrict ourselves to the region $0.1 < k < 0.65$ (Figure 3), because inside the blobs the chain is rather free and no change to non-Rouseian behavior can be expected. Figure 8 shows a semilogarithmic plot of $S_n(k,t)$ vs. $^1/_6 l^2k^2(wt)^{1/2}$ for the system where all chains are mobile. The data clearly give a common curve as expected from the Rouse model until $t \gtrsim 10^5$, which is approximately the time where global diffusion occurs. For $t > 10^5$, the correlation drastically breaks down, as shown by the data for $k = 0.1$ and $k = 0.2$. The results are in excellent agreement with former Monte Carlo and experimental results.[33] Our new calculations extend their results to much larger values of $k^2l^2(wt)^{1/2}$. Again no evidence of reptation, where one expects a very different behavior, can be seen. For $d_T^{-1} > k/2\pi > \langle R_G^2\rangle^{-1/2}$, one expects after de Gennes[11]

$$N^2S(k,t) = \bar{S}(k) + NN_e f(l^2k^2(wt)^{1/2}) \tag{26a}$$

with

$$\bar{S}(k) = S(k,0) \exp\{-(kd_T/6)^2\}$$

and

$$f(x) \propto \tfrac{1}{3} - c_0 x, \quad x \ll 1$$
$$\propto c_1/x, \quad x \gg 1 \tag{26b}$$

This gives

$$S_n(k,t) = \exp\left\{\frac{-k^2 d_T^2}{36}\right\} + \frac{NN_e}{S(k,0)} f(l^2k^2(wt)^{1/2}) \tag{27}$$

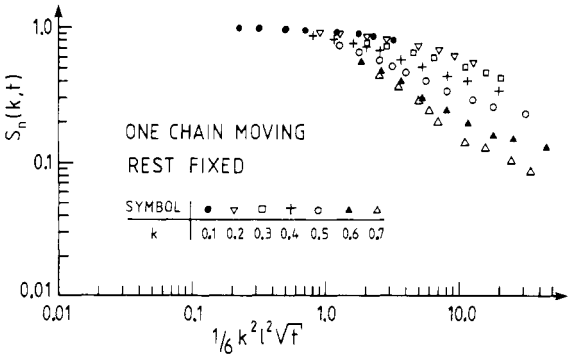

Figure 9. $S_n(k,t)$ of the single chain in a frozen environment vs. $^1/_6 k^2 l^2 t^{1/2}$ in a log–log plot.

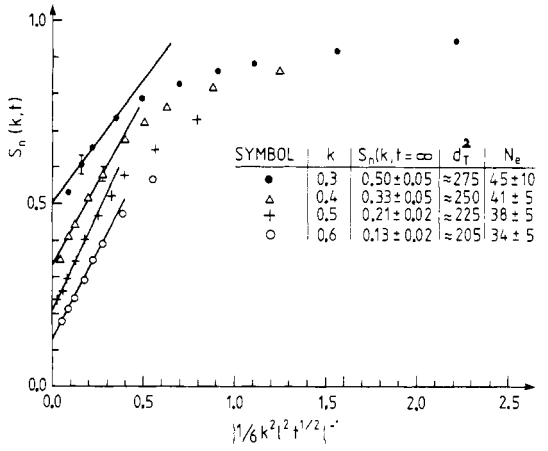

Figure 10. Extrapolation of $S_n(k,t)$ for the single mobile chain in the frozen environment to $x \to 0$ with $x = \{^1/_6 k^2 l^2 t^{1/2}\}^{-1}$ to estimate d_T^2 and N_e. The results of N_e using $d_T^2 = 2l^2 N_e$ (NRRW formula) and $d_T^2 = l^2 N^{1.18}$ coincide within the errors.

In Figure 9 we show the results for the mobile chain in a frozen environment, which are in good agreement with eq 26. For $x = l^2 k^2 (wt)^{1/2} \to \infty$, we arrive at $S_n(k,t) = \exp\{-(k^2 d_T^2/36)\}$. In Figure 10 the data of Figure 9 are extrapolated to $x \to \infty$. Using $d_T^2 \approx 6N_e$, one gets an additional estimate of N_e. The values are given in the table of Figure 10. They are, in contradiction to the theory, clearly k dependent but qualitatively agree with the results of N_e taken from the different time regimes of $g_1(t)$. Our results hence imply that reptation occurs for a frozen-in environment but does not occur if the environment is mobile, under otherwise identical conditions. This implies the tube diameter cannot be a consequence of geometrical constraints alone.

The above-mentioned theory of de Gennes[11] is based on the idea that for $t < \tau_R$ ($=\tau_1 N^3/N_e$) density fluctuations inside the tube are very small. If one now introduces explicitly the assumption that for $t > \tau_d$ ($=\tau_1 N^2$) two monomers i and j inside the chain ($i \neq j$, $1 \ll i, j \ll N$) move for the same time over the same distance, one arrives after a scaling assumption at a very different formula[13]

$$S_n(k,t) = \exp(-F\{k^2 l^2 (wt)^{1/4}\}) \qquad (28)$$

with $F > 0$ and $F(x) \propto x$ for $x \gg 1$. Figure 11 shows a plot of this scaling form. The strong line corresponds to the desired exponential behavior. The data of the reptative system only give a common curve for $t < \tau_d$ and not for $t > \tau_d$ as expected from eq 28. The crossover toward constant values for $t > \tau_d$ seen in Figures 9 and 11 imply that the structure factor settles down at the appropriate values following from the mean monomer density inside a tube as given by eq 26a and Figure 10.

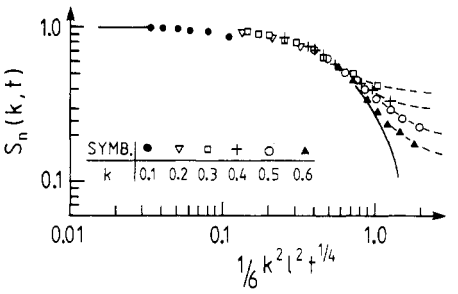

Figure 11. Double-logarithmic plot of $S_n(k,t)$ vs. the modified scaling variable $^1/_6 k^2 l^2 t^{1/4}$ (after ref 13). The full line gives qualitatively an exponential behavior.

V. Conclusions

The previous sections contain three results. With respect to static properties, we found strong numerical evidence for the equality of the values and not only the power laws of the mean square end-to-end distance for melts and for isolated chains at $T = \Theta$ (eq 11). The prefactor is larger than the result for simple random walks by the factor 2.20. It is an interesting problem for future work to give more precise estimates of this factor for the diamond lattice as well as for other lattices and to look for its (probably) systematic coordination number dependence.

Our *main* result concerns the dynamics of melts. Here, we find, even for a system which with regard to static properties should be a good candidate for reptative behavior, *no* onset of reptation. Even if one considers the estimated tube diameters $d_T \approx 30$–50 Å for the smallest systems, where $\tau_R \propto N^{3.3}$ [16,31] occurs, our system still is a good candidate for reptation. For the very flexible PDMS, we estimate the typical length of a bond as $l \gtrsim 3$ Å (using $\langle R^2(N,\Theta)\rangle$ of ref 23). Taking into account that a lattice bond should represent at least ≈3 real bonds, the diameter $d_T \approx 30$–50 Å corresponds to 3–6 effective bond lengths. This gives in our present units (note $l^2 = 3$) $d_T^2 \approx 30$–120 and $N_e \approx 5$–20. Thus the simulated system represents also from this point of view a "reptation system". In addition, our chains represent significantly longer effective chains compared to the shortest PDMS chains ($M_w = 15\,000$), for which $\eta \propto M^{3.3}$ [36] was found. This was taken as a "proof for reptation". For the mean square displacements, we cover the whole time regime from initial diffusion of a single monomer to the final diffusion of the whole chain. A similar result is given by the time-dependent coherent structure function $S_n(k,t)$. $S_n(k,t)$ clearly shows Rouse-like behavior, in excellent agreement with the results of previous simulations and neutron spin-echo measurements.[13-15,33] Our present data are able to extend the results to much higher values of the argument $^1/_6 l^2 k^2 \cdot (wt)^{1/2}$. In light of these results, a recent critique[16,18] on the mentioned previous data is not supported. Especially, it is clear that a recent simulation by Deutsch,[18] where he claims to find reptation for a melt, cannot prove melt properties. As shown in ref 19, he has artificially built in the reptation mechanism into his algorithm by allowing chains to overlap with themselves but not with other chains. In conclusion, if reptation occurs in a melt anywhere, the onset of reptation is shifted to much higher densities and much longer chains than thought before. If so, a microscopic theory for estimating d_T is needed. At the same time the Rouse model is only able to explain qualitatively a few properties of polymeric melts, while other properties, even in experiments, give very different results ($\tau_R \propto N^{3.3}$ instead of $\tau_R \propto N^2$).[34] Therefore it is one of the most important future tasks of polymer statistics

to develop an extensive theory of the dynamics of polymer melts for the most usual chain lengths and concentration regimes.

Even if reptation does not occur in melts at all, nevertheless the reptation model would be important for many polymer problems, such as short chains in a melt of very long chains or the problem of a single mobile chain in a network. Therefore even the data of the moving chain in the frozen environment are carefully analyzed. It turns out that the available theories of $S_n(k,t)$ and $g(t)$[10,11,13] have a rather qualitative character. It is necessary to find a more quantitative theory, especially for the connections between the two different scaling formulations ($x \propto k^2t^{1/2}$ or $x \propto k^2t^{1/4}$) and for the full crossover from Rouse-like to reptative behavior.

Acknowledgment. The author thanks Professor K. Binder for many valuable discussions and critical reading of the manuscript. He also thanks A. Baumgärtner for pointing out the questions investigated in section III. In addition, the referees are thanked for pointing out references pertaining to the statics.

References and Notes

(1) B. Duplantier, *J. Phys. (Paris)*, **43**, 991 (1982).
(2) K. Kremer, A. Baumgärtner, and K. Binder, *J. Phys. A: Math. Gen.*, **15**, 2879 (1982).
(3) See, e.g., P.-G. de Gennes, "Scaling Concepts in Polymer Physics", Cornell University Press, Ithaca, NY, 1979.
(4) P. E. Rouse, *J. Chem. Phys.*, **21**, 1272 (1953).
(5) B. Zimm, *J. Chem. Phys.*, **24**, 269 (1956).
(6) J. D. Ferry, R. F. Landel, and M. L. Williams, *J. Appl. Phys.*, **26**, 359 (1955). F. Bueche, "The Physical Properties of Polymers", Interscience, New York, 1962.
(7) S. F. Edwards and J. W. V. Grant, *J. Phys. A: Math. Gen.*, **6**, 1169, 1186 (1973).
(8) P.-G. de Gennes, *J. Chem. Phys.*, **55**, 572 (1971).
(9) M. Doi and S. F. Edwards, *J. Chem. Soc., Faraday Trans. 2*, **74**, 1789, 1802, 1818 (1978).
(10) P.-G. de Gennes, *J. Chem. Phys.*, **72**, 4756 (1980).
(11) P.-G. de Gennes, *J. Phys. (Paris)*, **42**, 735 (1981).
(12) J. Klein, *Nature (London)*, **271**, 143 (1978); *Macromolecules*, **11**, 852 (1978).
(13) A. Baumgärtner and K. Binder, *J. Chem. Phys.*, **75**, 2994 (1981).
(14) M. Bishop, D. Ceperly, H. L. Frisch, and M. H. Kalos, *J. Chem. Phys.*, **76**, 1557 (1982).
(15) D. Richter, A. Baumgärtner, K. Binder, B. Ewen, and J. B. Hayter, *Phys. Rev. Lett.*, **47**, 109 (1981).
(16) P.-G. de Gennes and L. Léger, preprint.
(17) J. P. Cohen-Addad, *J. Phys. (Paris)*, **43**, 1509 (1982).
(18) J. M. Deutsch, *Phys. Rev. Lett.*, **49**, 926 (1982).
(19) K. Kremer, JÜL-Report 1832 (1983), available from ZB der Kernforschungsanlage Jülich, D-5170 Jülich, West Germany.
(20) M. Daoud and G. Jannink, *J. Phys. (Paris)*, **37**, 973 (1976).
(21) C. Domb and M. E. Fisher, *Cambridge Philos. Soc.*, **54**, 2118 (1966).
(22) P. G. Khalatur, S. G. Pletneva, and Yu. G. Papulow, *J. Phys. (Paris), Lett.*, **43**, L683 (1982).
(23) R. G. Kirste and B. R. Lehnen, *Makromol. Chem.*, **177**, 1137 (1976).
(24) M. L. Mansfield, *J. Chem. Phys.*, **77**, 1554 (1982).
(25) J. G. Curro, *J. Chem. Phys.*, **61**, 1203 (1974).
(26) F. T. Wall and W. A. Seitz, *J. Chem. Phys.*, **67**, 3722 (1977).
(27) J. G. Curro, *Macromolecules*, **12**, 463 (1979).
(28) E. De Vos and A. Bellemans, *Macromolecules*, **7**, 812 (1974); **8**, 651 (1975)
(29) M. Bishop, D. Ceperly, H. Frisch, and M. Kalos, *J. Chem. Phys.*, **72**, 3228 (1980).
(30) P.-G. de Gennes, *Macromolecules*, **9**, 587, 594 (1976).
(31) W. W. Graessley, *J. Polym. Sci., Polym. Phys. Ed.*, **18**, 27 (1980).
(32) P.-G. de Gennes, *Physics (N.Y)*, **3**, 37 (1967).
(33) D. Richter, A. Baumgärtner, K. Binder, B. Ewen, and J. B. Hayter, *Phys. Rev. Lett.*, **48**, 1695 (1982).
(34) K. Osaki and M. Kurata, *Macromolecules*, **13**, 671 (1980).
(35) K. Kremer, *Z. Phys. B*, **45**, 149 (1981).
(36) T. Kataoka and S. Ueda, *J. Polym. Sci., Part A*, **5**, 973 (1967).
(37) K. E. Evans and S. F. Edwards, *J. Chem. Soc., Faraday Trans. 2*, **77**, 1891 (1981).

Polymer–Polymer Diffusion in Melts

Françoise Brochard,* Jacqueline Jouffroy, and Paul Levinson

Collège de France, Physique de la Matière Condensée,† 75231 Paris Cedex 05, France.
Received January 10, 1983

ABSTRACT: The mutual diffusion coefficient for a miscible binary polymer mixture is strongly dependent on the composition of the mixture. This leads to very unusual concentration profiles. For two pure A and B blocks in contact at time $t = 0$, we predict a concentration profile $\phi_t(x)$ linear in the spatial coordinate x. The region of mixing should not have a diffuse tail, but has a finite size $2(D_0t)^{1/2}$. These features are attenuated if we start not from pure A and B but from an A-rich sample against a B-rich sample.

I. Introduction

Compatible polymers are largely studied because of the mechanical properties offered by blends of two (A and B) polymers. It is difficult to find two polymers that are compatible on a microscopic scale. In the liquid state, the free energy F of the A–B mixture is well described by Flory–Huggins theory. Per site, F is given by

$$\frac{F}{kT} = \frac{\phi}{N_A} \ln \phi + \frac{1-\phi}{N_B} \ln (1-\phi) + \chi\phi(1-\phi) \quad (1)$$

where ϕ is the volume fraction of A and N_A and N_B are the degree of polymerization of A and B. From (1), one can derive the critical value of χ for segregation of A and B. In the symmetrical case ($N_A = N_B$), $\chi_C = 2/N$. For most A–B polymer pairs, χ is positive and larger than χ_C, and segregation occurs. The few cases that mix[2] are (a) almost chemically identical species (e.g., deuterated–nondeuterated pairs) and (b) some A–B pairs with specific interactions giving $\chi < 0$ (corresponding to a negative enthalpy of mixing). There is a growing interest in the *dynamics* of fluctuations in blends.[1,3] Our purpose here is to study the mutual penetration of two miscible polymers A and B. At time $t = 0$, consider that two liquid but viscous blocks of pure A and pure B are put into contact and examine the concentration profile $\phi(x,t)$ at later times t, assuming a negative interaction parameter χ *independent of* ϕ. This type of mixing has been studied by spectroscopic techniques.[4] In the standard interpretation of the data, the mutual diffusion coefficient D is supposed

† Équipe de recherche associée au CNRS (No. 542).

0024-9297/83/2216-1638$01.50/0